Applied Physics Letters ARTICLE scitation.org/journal/apl

Phase-sensitive imaging of microwave currents in superconductive circuits

Cite as: Appl. Phys. Lett. **114**, 232601 (2019); doi: 10.1063/1.5109726
Submitted: 11 May 2019 · Accepted: 15 May 2019 ·
Published Online: 10 June 2019

A. Karpov,[1,a)] A. P. Zhuravel,[2] A. S. Averkin,[1] V. I. Chichkov,[1] and A. V. Ustinov[1,3,4]

AFFILIATIONS

[1]National University of Science and Technology MISIS, 119049 Moscow, Russia
[2]B. Verkin Institute for Low Temperature Physics and Engineering, NAS of Ukraine, 61103 Kharkov, Ukraine
[3]Physikalisches Institute, Karlsruhe Institute of Technology (KIT), 76131 Karlsruhe, Germany
[4]Russian Quantum Center, 100 Novaya Street, Skolkovo, Moscow Region 143025, Russia

[a)]**Author to whom correspondence should be addressed:** alexandre.karpov@yahoo.com

ABSTRACT

We propose an improved measuring technique for microwave currents in superconductive circuits, demonstrate it experimentally, and validate the experimental data with numerical simulations. Contemporary superconductive electronics widely uses planar circuits with micrometer-scale elements for a variety of applications. With the rise of complexity of a circuit and increase in the number of its components, a simple impedance measurement is often not efficient for the diagnosis of problems, nor for clarifying the physics underlying the circuit response. The established Laser Scanning Microscopy (LSM) technique generates micrometer-scale images of the amplitude of the microwave currents in a planar superconductive circuit, but not the phase of the oscillating currents. Here, we present a more powerful type of LSM imaging containing signal phase information. We employ a fast-optical modulator in order to synchronize the phase of the laser intensity oscillation with the phase of the probing microwave signal. The loss induced in a laser illuminated area strongly depends on the phase difference between the RF probing signal and the laser beam modulation. As a proof of concept, we present the phase-sensitive LSM measurements of the inner mode currents in a planar superconductive resonator and confirm the data with numerical simulation of the resonator's electrodynamics.

The low-current superconductive electronics widely employs planar thin-film circuits for a variety of applications. To mention a few, these are devices for quantum metrology, quantum computing, ultrasensitive terahertz detectors, SQUID magnetometers, etc.[1–3] With the rise of complexity of circuits and increasing number of components, a simple impedance measurement may not be efficient for verifying circuit functionality. Employing spatially resolved techniques for imaging microwave currents makes it possible to better understand circuit operation regimes and their properties. In this respect, Laser Scanning Microscopy (LSM) is a potential tool for imaging the RF current distributions in planar superconducting circuits with micrometer-scale resolution. The currently available LSM technique provides information on the local amplitude of the microwave currents in a circuit, but not the phase of these currents.[4,5] Making LSM imaging phase sensitive would significantly improve the understanding of the dynamics of interactions between different parts of the circuit and may allow for detecting complex modes of oscillations therein. Demonstration of a proof of concept of the phase-sensitive LSM operation is the purpose of this work.

The existing LSM technique employs a focused laser beam for scanning the surface of a superconducting circuit. In the area illuminated by the laser beam, superconductivity is locally depressed by generation of quasiparticles due to breaking of the Cooper pairs (photoresponse) and by the heating effect of the laser radiation. The combined effect of laser radiation and the microwave signal is the AC loss proportional to the square of the amplitude of the RF current in the illuminated area.[4] In a typical LSM measurement, the transmitted (or reflected) microwave signal amplitude is registered and mapped as a function of the XY laser beam position, effectively resulting in imaging of the amplitudes of the microwave currents in the circuit.

The central idea of this work is to develop a more powerful type of LSM measurement depicting signal phase information. We are using a fast-optical modulator for synchronizing the oscillations of the laser intensity with the frequency of the probing microwave signal. The loss induced in the laser illuminated area of the superconductive circuit is strongly dependent on the phase

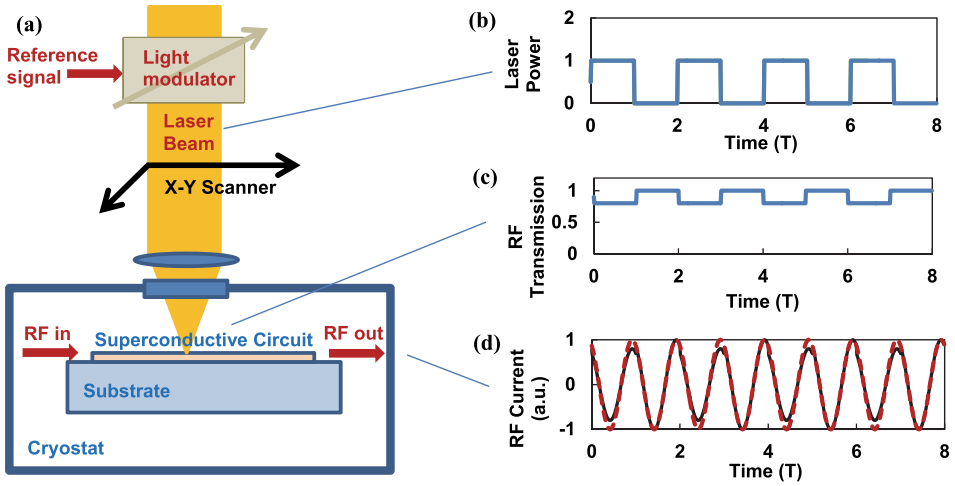

FIG. 1. Laser scanning microscopy schematics. The LSM setup is identical to that reported in Ref. 4, except that the light modulator is inserted between the laser source (640 nm) and the microscope optics. (a) Detection of the LSM signal: A microwave signal at frequency f is transmitted through the superconductive planar circuit installed in a cryostat with an optical window. The laser beam is focused on the surface of the superconductive circuit at the position X_1Y_1 controlled by the X-Y scanner. (b) The laser beam intensity is pulse-modulated at the frequency $f/2$ phase-locked with the RF source. (c) The time profile of the loss induced by the laser beam follows the beam intensity modulation, resulting in a small variation in the output RF signal. (d) The dotted line is the input signal and the continuous line is the output signal of the superconductive circuit. As a result of parametric interaction in the illuminated area, a signal is generated at the differential frequency ($f/2$) of the RF signal and the laser modulation frequency. The I and Q components of the signal at $f/2$ are measured with a lock-in amplifier and are used to determine the phase and the amplitude of the RF signal. Mapping of the amplitude and phase over the superconductive microcircuit is made with the help of an X-Y scanner. The details of the RF to sample connection are pictured in Fig. 2(b).

difference between the RF probing signal and the phase of the laser beam modulation.

The detection mode of the microwave signal is essential for obtaining the LSM response. In the traditional (scalar) LSM, the transmission of the microwave signal is modulated at a relatively low frequency f_M by pulse-driving the laser power supply. The amplitude of the induced pulsation of the microwave signal at the frequency f_M is measured at the circuit output with a lock-in amplifier employing the signal driving the laser power as the reference signal. The amplitude at the lock-in-phase (I) output constitutes the LSM response.[4]

For the phase-sensitive LSM mode described here, we use the same reference oscillator to phase-lock the microwave signal source and the laser beam power modulation. As a simple example, let us consider LSM operation with the microwave signal in the superconductive circuit oscillating at the frequency f with the phase φ, and the laser beam pulse-modulation at the frequency $f_M = f/2$ with the phase equal to zero (Fig. 1). While the $f/2$ frequency component is absent in the spectrum of the incoming microwave signal, it will be present at the circuit output port due to modulation of the circuit transmission by the laser beam power. The parametrically generated $f/2$ signal will thus be detected with a lock-in amplifier using the driving signal of the laser beam modulator as a reference. Normally, only a small part of the superconductive circuit is affected by the laser beam, and therefore the signal $a(t)$ is only slightly dimmed by the applied laser power by a small factor $\alpha \ll 1$ corresponding to the scalar LSM response amplitude. The signal at the superconductive circuit may be written as:

$$a(t) = (1 - \alpha b(t))\sin(2\pi f t + \varphi), \tag{1}$$

where $b(t)$ is the unitary rectangular pulse train with the frequency $f_M = f/2$ [Fig. 1(b)] that can be represented as a sum

$$b(t) = \frac{4}{\pi}\left(\sin\left(\frac{2\pi f}{2}t\right) + \frac{1}{3}\sin\left(3\frac{2\pi f}{2}t\right) + \frac{1}{5}\sin\left(5\frac{2\pi f}{2}t\right) + \cdots\right). \tag{2}$$

Substituting (2) into (1), we obtain:

$$a(t) = \left(1 - \alpha\frac{4}{\pi}\left(\sin\left(\frac{2\pi f}{2}t\right) + \frac{1}{3}\sin\left(3\frac{2\pi f}{2}t\right) + \frac{1}{5}\sin\left(5\frac{2\pi f}{2}t\right) + \cdots\right)\right)\sin(2\pi f t + \varphi), \tag{3}$$

where the $f/2$ spectral component of the microwave signal $a(t)$ may be represented as a sum of in-phase and quadrature components I and Q that we measure at the I and Q outputs of the lock-in amplifier in the LSM experiment

$$a_{f/2}(t) = I\cos\left(\frac{2\pi f}{2}t\right) + Q\sin\left(\frac{2\pi f}{2}t\right) = \alpha\frac{2}{3\pi}\left\{2\cos\left(\frac{2\pi f}{2}t\right)\cos(\varphi) - \sin\left(\frac{2\pi f}{2}t\right)\sin(\varphi)\right\}, \tag{4}$$

or

$$I = \alpha\frac{4}{3\pi}\cos(\varphi) \quad \textit{and} \quad Q = \alpha\frac{2}{3\pi}\sin(\varphi). \tag{5}$$

The values of I and Q of the $f/2$ component in the microwave spectrum are directly measured in experiment at the LSM with a lock-in amplifier. Both I and Q are proportional to the induced loss factor α, and the phase φ is equal to the phase of the RF signal at frequency f in the area illuminated by the focused laser beam. Using Eq. (5), the amplitude and the phase of the RF signal in the superconductive circuit may be calculated from the measured I and Q values.

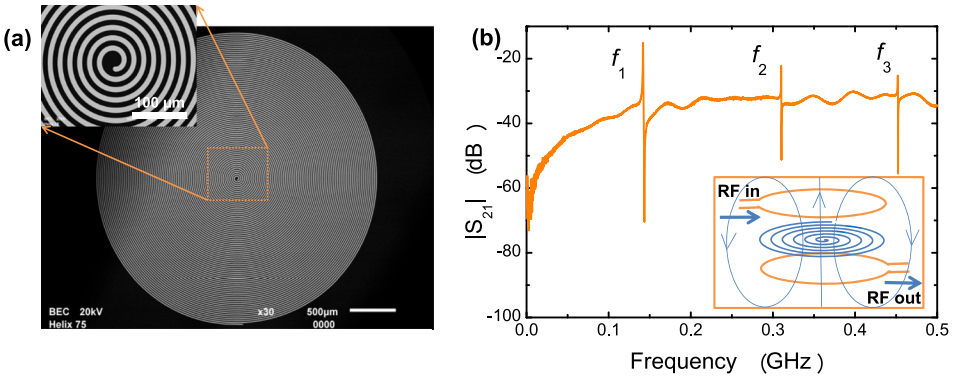

FIG. 2. (a) Planar superconductive resonator shaped as an Archimedean spiral. The spiral diameter is 2.88 mm. The spiral line and spacing are 10 mm wide and the NbN film is about 10 nm thick. (b) The measured spectrum of the inner modes of the spiral. The spiral is connected to the microwave lines through two coupling loops, as shown in the insert. At the spiral resonance frequency, the loop-to-loop magnetic coupling (S_{21}) peaks. The resonance frequencies of the first three modes scale approximately in the proportion 1:2:3 (143 MHz, 309 MHz, and 452 MHz).

If we study the RF current distribution of the inner modes in a planar weakly coupled resonator, the LSM data should be relatively simple and, with appropriate reference, the phase φ of the RF oscillations will be 0 or π. Consequently, the Q component will be close to zero, when the component I from (5) will be changing the sign at the antinodes of the standing wave. The sign inversion at the adjacent nodes would not be possible to detect with traditional scalar LSM. Demonstration of this particular effect is used as a proof of concept in our work.

For the experimental demonstration of a phase-sensitive LSM operation, we use a superconductive distributed resonator formed by a planar Archimedean spiral with multiple inner modes shown in Fig. 2(a). The resonator can be excited by the magnetic RF field perpendicular to its plane. We use the two current loops terminating the input and output coaxial lines as LSM signal ports, as described in Refs. 6 and 7 [see also the icon in Fig. 2(b)]. The spectrum of inner modes of an Archimedean spiral is normally described by the following harmonic rule:[8]

$$f_n = \frac{nl}{c}, \tag{6}$$

where l is the total length of the resonator spiral line, c is the speed of light in the media, and n is the mode number ($n = 1, 2, 3\ldots$). Moreover, it was also found that the radial profile of the inner modes follows a simple expression

$$I_n(r/R_e) = I_{max}\sin\left(\pi n (r/R_e)^2\right), \tag{7}$$

with its precision better than 5%.[8] Here, I_n is the amplitude of microwave current of the inner mode number $n = 1, 2, 3\ldots$, R_e is the external radius of the Archimedean spiral, and r is the radial distance from the center of the spiral.

For LSM verification, we fabricated a compact NbN spiral resonator at the sapphire substrate shown in Fig. 2(a). Here, the Archimedean spiral has 72 turns with an external radius of $R_e = 1.44$ mm. The spiral line is 10 mm wide and about 10 nm thick. The LSM imaging of the current waveform of the standing waves was performed at the resonance frequencies of the spiral in a liquid helium cryostat described in Ref. 4. The spiral is inserted into a microwave line between two weakly coupled magnetic coils, as shown in the inset of Fig. 2(b). At the frequencies of spiral resonances, the loop-to-loop coupling peaks.[6,7] The measured spectrum of the inner modes of the spiral is presented in Fig. 2(b). The resonance frequencies of the first three modes are harmonically related in proportion close to 1:2:3, as in Eq. (6), and were excited at about 143 MHz, 309 MHz, and 452 MHz. It has been reported that in the NbN films as thin as in our experiment, the electron-phonon relaxation time is relatively short, on the order of 10–20 of picoseconds,[9] much faster than the signal oscillations in the present experiment, and we could ignore relaxation time effects for now. A more detailed simulation of the NbN resonator with HFSS (ANSYS High Frequency Structure Simulator) presented below shows that the kinetic inductance in the NbN film affects the resonance frequencies of the sample, reducing the resonance frequencies by about 30% in respect of Eq. (6).

The LSM images of the RF currents of the first three modes of the spiral resonator measured with the phase sensitive (bottom line) and conventional[4] (top line) LSM operation modes are presented in Fig. 3. We are using the same setup of the LSM as in Ref. 4, except for the light modulator (AM635) inserted between the laser (10 μW at

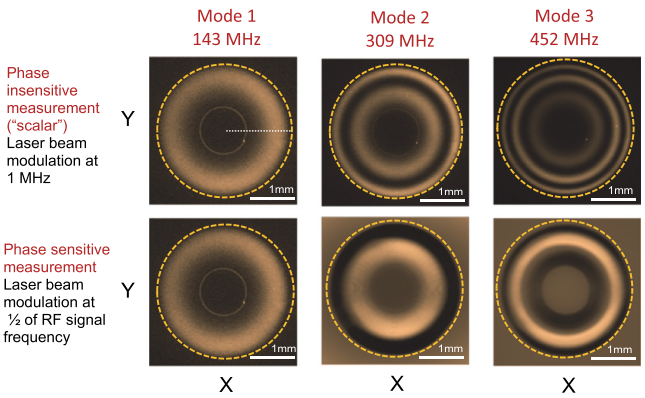

FIG. 3. LSM imaging of the X-Y distribution of RF currents at the 1–3 inner modes of the spiral resonator pictured in Fig. 2. The phase-sensitive LSM images are in the bottom line and the traditional LSM images[4,8] are in the top line. The plotted value is the in-phase component I at the LSM lock-in amplifier output [Eq. (5)]. The LSM field of view is about 4 × 4 mm and the spiral diameter is 2.88 mm (dashed line). The individual spiral turns are not fully resolved because the wide field LSM optics spatial resolution is less than 20 mm. The image coloring ranges from bright (higher LSM response amplitudes) to a color darker than the image background (negative LSM response). A bright spot indicates a short between the two turns of the spiral. Notably, the images of the first mode current distribution are identical, while for the second and third modes they differ. The phase-sensitive LSM images of the second and third modes demonstrate the contrast inversion in the adjacent antinodes.

640 nm) and the LSM optics. The plotted value is the measured in-phase component I at the LSM lock-in amplifier output (SR844). In this experiment, at each resonant frequency, the phase reference at the lock-in amplifier was adjusted to maximize the component I output, putting Q close to zero. The measured 2D distributions of RF currents in the first three modes in the spiral superconductive resonator are center-symmetric and present a combination of circular nodes and antinodes. The individual spiral turns are not fully resolved because the wide field LSM optics spatial resolution is less than 20 mm. A bright spot indicates a short between the two turns of the spiral, showing an ease for detecting anomalies in complex superconductive circuits with LSM. In the phase-sensitive mode, the short is visible when the data are taken with a better space resolution, see Fig. 4(e). The coloring in the images of Fig. 3 ranges from bright (higher LSM response amplitudes) to a color darker than the image background (negative LSM response). In phase-insensitive, conventional measurements, the laser beam is modulated at low frequency (1 MHz), while in the phase-sensitive regime the beam is pulse-modulated at $^1/_2$ of the microwave signal frequency (i.e., at $f_n/2$). Notably, the images of the first mode are identical, while in the second and third modes they differ. The latter two images demonstrate the phase inversion in the adjacent antinodes, confirming the expected operation in the LSM phase-sensitive mode.

Moreover, we checked the phase-sensitive LSM measuring technique by tracing the radial profile of the inner modes of the spiral resonator along the dotted line, as shown in Fig. 3 upper left icon. We did an LSM radial scan with a higher optical resolution objective, giving micrometer-scale spatial resolution and allowing detecting LSM response of the individual turns of the spiral line in resonator. Figure 4 presents radial line scans of the second and third modes in a spiral resonator at frequencies 309 MHz and 451 MHz, respectively, measured at the in-phase LSM lock-in amplifier output I, and normalized to get the maximum amplitude equal to 1. The LSM response peaks at the crossings of the spiral turns and is close to zero between them. The phase-sensitive LSM data are shown in the bottom [Figs. 4(c) and 4(d)] and the conventional phase-insensitive data are presented in the top row [Figs. 4(a) and 4(b)]. As in the Fig. 3 data, for phase-insensitive measurements, the light beam is modulated at a low frequency of 1 MHz, and in the phase-sensitive regime, the laser beam is pulse-modulated at $^1/_2$ of the microwave signal frequency. The envelope of the measured curves [Figs. 4(c) and 4(d)] resemble the model predictions given by Eq. (7). The phase inversion at the adjacent antinodes is clearly visible as alternation of the sign of the LSM signal in Figs. 4(c) and 4(d). The conventional scalar LSM signal shown in Figs. 4(a) and 4(b) produces a nearly identical profile, but without change of the phase.

The measured phase-sensitive LSM data have been verified in more detail with numerical HFSS simulation of the current distribution in the 2nd and 3rd modes of the spiral resonator. In the HFSS

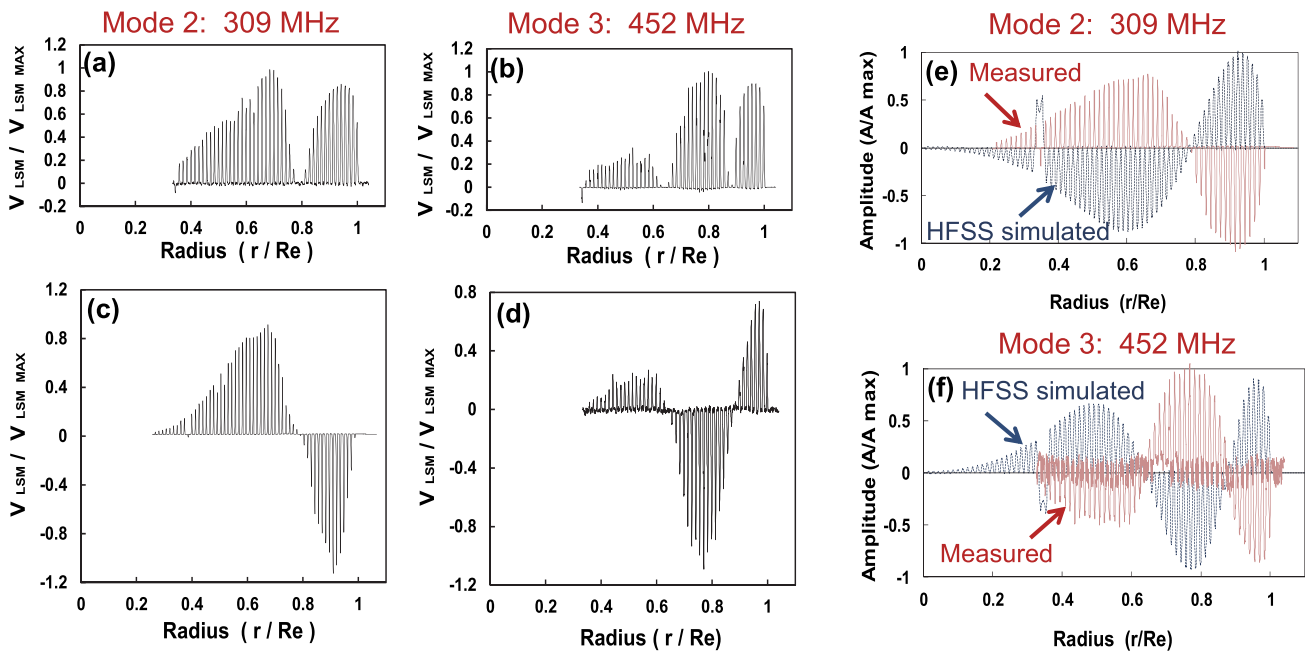

FIG. 4. Radial LSM scan of the RF current waveform of 2nd and 3rd inner modes of the spiral resonator. The scan is made along the dotted line of Fig. 3, upper left, at 309 MHz (a) and (c) and 451 MHz (b) and (d), respectively. The data in (a)–(d) are the LSM response voltage measured at the in-phase output of the lock-in amplifier. The phase-sensitive LSM data are in the bottom row (c) and (d) and the phase-insensitive data are in the top row (a) and (b). The LSM response voltage is normalized to the maximum value. The individual spiral turns are resolved, making narrow spikes in LSM response. The phase inversion at the adjacent antinodes is well visible when measured with the proposed phase-sensitive version of the LSM. In (e) and (f), the RF currents' HFSS simulation (dotted line) is compared with the measured LSM data. For image clarity, the sign of the HFSS simulated curves is inverted against the measured data. In (e) and (f), the measured amplitude of RF currents is obtained as a square root of the LSM voltage.[4] The accidental short between the spiral turns is included in the HFSS model. The HFSS calculated curve shapes and nodes' positions match well with the observed in-phase-sensitive LSM data (e) and (f), validating the measurement technique.

model of the spiral resonator, the kinetic inductance per square of the NbN film is 0.015 nH/□, consistent with the penetration depth of about $\lambda = 340$ nm. The defect in the sample, a short between the spiral turns in the central area, is taken into account. The measured and the HFSS generated radial profiles of the currents of the resonator inner modes are displayed in Figs. 4(e) and 4(f). Here, the HFSS simulated data are drawn with a dotted line (the top curve at the edge of the spiral at $r/R_e = 1$). For better perception, in order to avoid a messy overlap of the curves, the sign is inverted in HFSS simulated against the measured profiles. The experimental amplitude of the RF currents is obtained as a square root of the absolute value of the measured LSM response.[4] All data in Fig. 4 are normalized to get the maximum amplitude equal to 1. The interwindings' shorting defect appears as a spike in the HFSS simulated current curves at $r/R_e = 0.35$. The departure from linearity of the LSM response would be visible from the mismatch in HFSS predicted and LSM measured radial scan envelopes, but is not noticeable in our data. The individual spiral turns are evident in both sets of data, giving a good reference for position. In LSM and HFSS data, the 2nd mode's node position is 14 turns away from the spiral edge, while for the 3rd mode the two nodes are located 9 and 25 turns away from the edge, respectively. The RF current curve envelopes and positions of the nodes calculated in the HFSS match well with the observed LSM data, and support the soundness of the proposed LSM technique.

In summary, in this work, we proposed and demonstrated experimentally a "phase-sensitive" LSM technique for the visualization of RF currents in superconductive microwave circuits. In order to obtain the phase contrast, we modulate the laser beam intensity at a frequency synchronized with a subharmonic of the microwave signal propagating through the circuit. The proposed technique for the phase-sensitive imaging of the microwave currents with micrometer-scale resolution opens ways to explore and understand a great variety of complex RF current distributions and microwave patterns in superconductive circuits. The final effect of the proposed experimental technique should be similar to the transition from scalar to vector network analyzers for microwave applications.

We would like to thank Steven M. Anlage for valuable discussions. We acknowledge the financial support of this work by the Volkswagen Foundation Grant No. 90284, by Grant Nos. 3.5490.2017/ВУ and 3.3360.2017/PH from the Ministry of Education and Science of Russian Federation, and also by Grant Nos. K2-2014-025 and K2-2017-081 in the framework of Increase Competitiveness Program of the NUST MISIS.

REFERENCES

[1]A. M. Zagoskin, *Quantum Engineering: Theory and Design of Quantum Coherent Structures* (Cambridge University Press, Cambridge, 2011), pp. 272–311.
[2]P. Jung, A. V. Ustinov, and S. M. Anlage, "Progress in superconducting metamaterials," Supercond. Sci. Technol. **27**, 073001 (2014).
[3]E. Brundermann, H.-W. Hubers, and M. F. Kimmitt, *Terahertz Techniques* (Springer, New York, 2012), p. 310.
[4]A. P. Zhuravel, A. G. Sivakov, O. G. Turutanov, A. N. Omelyanchouk, S. M. Anlage, A. Lukashenko, A. V. Ustinov, and D. Abraimov, "Laser scanning microscopy of HTS films and devices," Low Temp. Phys. **32**, 592 (2006).
[5]C. C. Chi, M. M. T. Loy, and D. C. Cronemeyer, "Optical probing technique for inhomogeneous superconducting films," Appl. Phys. Lett. **40**, 437 (1982).
[6]C. Kurter, A. P. Zhuravel, J. Abrahams, C. L. Bennett, A. V. Ustinov, and S. M. Anlage, "Superconducting RF metamaterials made with magnetically active planar spirals," IEEE Trans. Appl. Supercond. **21**, 709 (2011).
[7]N. Maleeva, M. V. Fistul, A. Karpov, A. P. Zhuravel, A. Averkin, P. Jung, and A. V. Ustinov, "Electrodynamics of a ring-shaped spiral resonator," J. Appl. Phys. **115**, 064910 (2014).
[8]N. Maleeva, A. Averkin, N. N. Abramov, M. V. Fistul, A. Karpov, A. P. Zhuravel, and A. V. Ustinov, "Electrodynamics of planar Archimedean spiral resonator," J. Appl. Phys. **118**, 033902 (2015).
[9]Y. P. Gousev, A. D. Semenov, G. N. Goltsman, A. V. Sergeev, and E. M. Gershenzon, "Electron-phonon interaction in disordered NbN films," Phys. B: Condens. Matter **194–196**, 1355–1356 (1994).